Applied Mathematics & Information Sciences
An International Journal

A Low PAPR Visible Light Communication System Employing SC-FDMA Technique

Young-Ju Kim[1], *Xun Li*[2]

[1]School of Information and Communication Engineering, Chungbuk National University, Chungbuk, 361-763, Republic of Korea
[2]Research and Innovation Center, Alcatel-Lucent Shanghai Bell, Shanghai, China

Received: 22 Sep. 2012; Revised 21 Oct. 2012; Accepted 11 Nov. 2012
Published online: 1 Mar. 2013

Abstract: White light emitting diode (WLED) technology has been regarded as an environment-friendly lighting in the future. The WLED lighting system is able to provide short range wireless communication while illuminating rooms. The WLED based visible light communication (VLC) systems employing orthogonal frequency division multiplexing access (OFDMA) technique has been investigated in many researches. However, the OFDMA technique has the inherent high peak-to-average power ratio (PAPR). Such a VLC system with high peak power produces flickering light that can be detected by human eyes uncomfortably. In this paper, the application of single carrier frequency division multiplexing access (SC-FDMA) to VLC system is proposed and investigated. Because of the lower PAPR, the VLC system employing SC-FDMA technique outperforms comparable systems employing OFDMA, considered in terms of bit error rate performance under various practical considerations. Moreover, the proposed system also protects LED devices and human's eyes from the over-bright due to peak signal power. Computer simulations corroborate the analysis results in the paper.

Keywords: Visible light communication, white LED, OFDM, single-carrier

1. Introduction

Light emitting diode (LED) offers many advantageous properties such as high brightness, reliability, lower power consumption and long lifetime. The LED is used in full color displays, traffic signals, and many other means of illumination. Recently, Indium gallium nitride (InGaN) based highly efficient blue and green LEDs have become commercially available. White light can be produced by mixing the three primary colors (red, green and blue). White light produced by such emitting diode (WLED) combinations is considered as a strong candidate for the future lighting technology. A short range visible light communication (VLC) system utilizing WLED also has been investigated in prior researches where the devices are used not only for illuminating rooms, but also for short range optical wireless communication [1-3]. These proposed technologies are gaining accelerating interest for applications in fast-growing markets such as industry automation, in-car communication, and home networking. The proposed systems have the following advantages: high power and distributed lighting equipment can reduce shadowing effect throughout a whole room; lighting equipment with white LEDs is easy to be installed and it is also aesthetically pleasing.

However, the use of WLEDs introduces a major disadvantage of low bandwidth with acceptable cost. Theoretically, the VLC system has infinite bandwidth without taking account with the cost of cost of production. In practical situation, by using discrete multi-tone transmission technique such as orthogonal frequency division multiplexing access (OFDMA), it has been shown that such bandwidth limitations can be overcome [4, 5]. Nevertheless, the OFDMA signal envelope has inherent high peak-to-average power ratio (PAPR) which makes the OFDMA signals suffering from in-band and out-band distortions due to non-linearity introduced at the transmitter diode. In VLC systems, the highly fluctuating envelopes also lead eye-safety problem and device lifetime problem since these envelopes produce high power and flicking light which can be detected by human eyes.

* Corresponding author: e-mail:yjkim@cbnu.ac.kr

In this paper, we propose a new VLC system employing single carrier frequency division multiplexing access (SC-FDMA) technique that has inherent low PAPR property. SC-FDMA utilizes single carrier modulation and frequency domain equalization [6-8]. It has similar performances and essentially the same overall structure as the OFDMA system, but much lower PAPR. Among the multiplexing methods of wireless communications, the SC-FDMA technique has been adopted by the 3GPP long term evolution (LTE) standard and its advanced version (LTE-A) as uplink multiple access scheme. We modify the structure of SC-FDMA technique for VLC system that reduces the complexity while producing real signal only. The real signal can be modulated directly and transmitted over emitting diode. We also derive the expression of the VLC system signals and analyze the PAPR. We compared the PAPR of the SC-FDMA with that of OFDMA using complementary cumulative distribution function (CCDF). Bit error rate (BER) performances are also compared under various considerations.

The remainder of this paper is organized as follows: Section 2 gives the modeling of optical wireless channel that is used in the analysis of this paper. In Section 3, an overview of the LED communication system and SC-FDMA are shown; we also derive the signal expression of the proposed system that integrates the LED transmission system. Section 4 presents the simulations results. Finally, conclusions are in Section 5.

2. Optical wireless channels

In this paper, the Monte Carlo ray-tracing algorithm is used to model the VLC system wireless channel. Every ray is generated at the emitter position with a probability distribution equal to its radiation pattern. The power of each generated ray is initially the normalized source power divided by the number of rays generated. When the reflection occurs, a new optical source is considered, and a new ray is generated with a probability distribution provided by the reflection pattern of the surface. This process continues during the simulation time. Finally, the power of the ray is reduced by the reflection coefficient (ρ) of the surface. Phong's model is used to describe the reflection pattern of surfaces [9]. Therefore, the total received power at the time t can be expressed by the following relationship

$$p(t) = \sum_{i=0}^{N_t-1} p_i(t), \tag{1}$$

where N_t is the number of rays arriving at the receiver at time t, and $P_i(t)$ is the power of i-th ray at the time. The channel impulse response is given by

$$h(t) = \sum_{k=0}^{K-1} p(t)\delta(t-k\Delta t), \tag{2}$$

where $K = t_{max}/\Delta t$, t_{max} denotes the maximum delay of the channel, Δt denotes the delay of specific channel. The noise is assumed to be an additive white Gaussian noise (AWGN). The channel impulse is assumed to be a Rayleigh fading component approximately. Thus, the received signal at the receiver by a photo diode without lens could be expressed by the following

$$\hat{x}(t) = h(t)x(t) + n(t), \tag{3}$$

where $\hat{x}$ represents the received signal current, $h(t)$ represents channel impulse, and $x(t)$ is the transmitted optical pulse and $n(t)$ is the AWGN component. In the frequency division multiplexing (FDM) systems, the signal could be expressed in matrix form as follows,

$$\begin{bmatrix} \hat{X}_1 \\ \hat{X}_2 \\ \vdots \\ \hat{X}_N \end{bmatrix} = H \begin{bmatrix} X_1 \\ X_2 \\ \vdots \\ X_N \end{bmatrix} + \begin{bmatrix} N_1 \\ N_2 \\ \vdots \\ N_N \end{bmatrix}, \tag{4}$$

where the capital letters in (4) is the frequency-domain representation of the variables in (3). For example, H is frequency domain channel response matrix and the subscript, N denotes the number of subcarriers in the FDM system.

3. WLED system employing SC-FDMA

3.1. Transceiver structure of the proposed system

SC-FDMA can be regarded as a discrete Fourier transform (DFT)-spread OFDMA. A block diagram of the WLED based VLC system with SC-FDMA is shown in Figure 1. The time domain data symbols are transformed to the frequency domain by an M-point DFT operation and subcarrier mapping has to be done before going through an N-point OFDM modulator, where N is much larger than M. When $Q = N/M$, Q denotes the band spreading factor. Users of an SC-FDMA system occupy different subcarriers in the frequency domain. The overall transmit signal becomes a single carrier signal with inherent low PAPR at the each user equipment. The transmit symbols are encoded by forward error correction (FEC) coding and interleaving to combat with the channel fading and noise caused bust errors. Many modulation schemes can be employed to generate complex symbols $\{c_k : k = 1,2,\cdots,K\}$.

Due to the characteristic of VLC systems, the complex symbols cannot be transmitted directly, thereby the signals sent to DC-bias block must be real symbols. Previous method in [4] is to add the complex conjugate of the mirror of the symbols to the latter before computing IFFT in OFDM modulator. This can be simplified to remove the image part of the modulated symbols c_k firstly, and add the image part to the latter to generate M symbols $\{d_m : m = 1,2,\cdots,M\}$, where $M = 2K$. The repacked time domain data are transformed to the frequency domain by

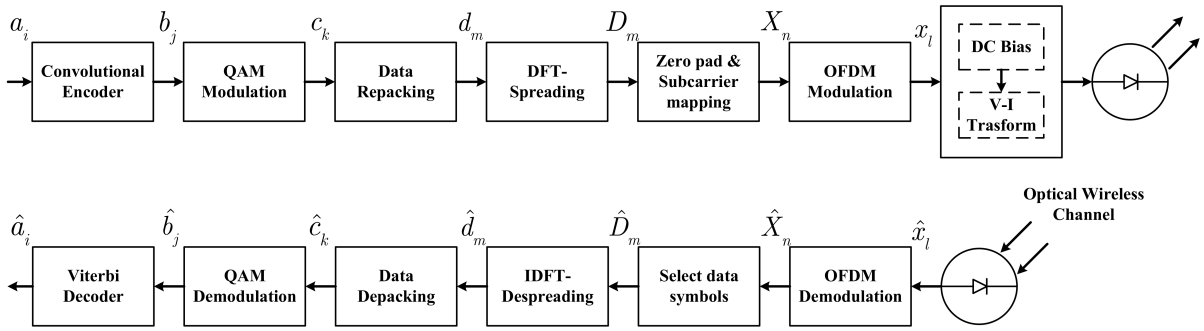

Figure 1 Block diagram of SC-FDMA WLED communication system

DFT block and the subcarrier mapping is done. The output symbols D_m is shown as the following

$$D_m = \sum_{p=0}^{M-1} d_p e^{-j2\pi \frac{p}{M} m}. \tag{5}$$

The signals after zero padding and subcarrier mapping can be expressed as the following for localized FDMA (LFDMA)

$$X_n = \begin{cases} D_m & 0 \le m \le M-1 \\ 0 & M \le l \le N-1 \end{cases}, \tag{6}$$

and for interleaved FDMA (IFDMA)

$$X_n = \begin{cases} D_{l/Q} & l = Qm \ (0 \le m \le M-1) \\ 0 & \text{otherwise} \end{cases}, \tag{7}$$

Note that, the symbols of LFDMA represent a user block in frequency domain, while the user's symbols of IFDMA are spread over all bandwidth as shown in Figure 2. Thereby the LFDMA subcarrier mapping algorithm is more feasible to design the multi-user and channel information feedback scheme for practical reasons. Finally, the OFDMA modulation can be expressed as follows

$$x_n = \frac{1}{N} \sum_{l=0}^{N-1} X_l e^{j2\pi \frac{l}{N} n}. \tag{8}$$

After the insertion of cyclic prefix, the real value baseband signal is modulated onto the instantaneous power of the optical carrier resulting in intensity modulation. The signals are biased before applying the signal for intensity modulation.

In optical systems, the real value baseband signal is modulated onto the instantaneous power of the optical carrier resulting in intensity modulation. The power amplifier is the last stage driving the antenna in radio frequency communication. However, it is changed in the LED based communication, as illustrated in Figure 3; the LED is biased before applying the signal for intensity modulation to avoid low power clipping. The biasing point should be carefully selected to account of the maximum allowable

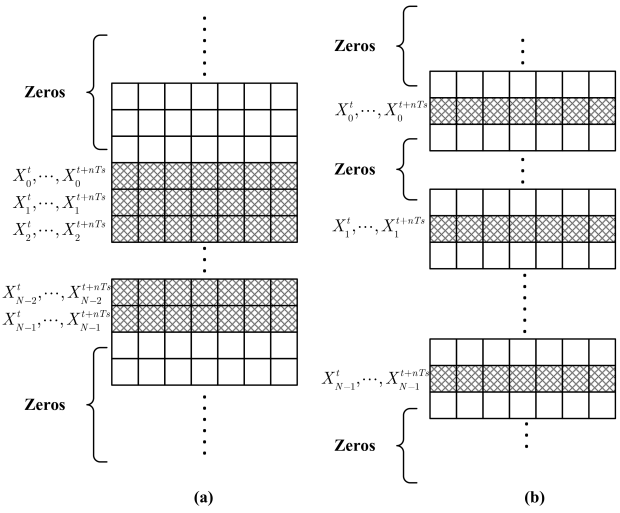

Figure 2 Subcarrier mapping: (a) Localized FDMA, (b) Interleaved FDMA

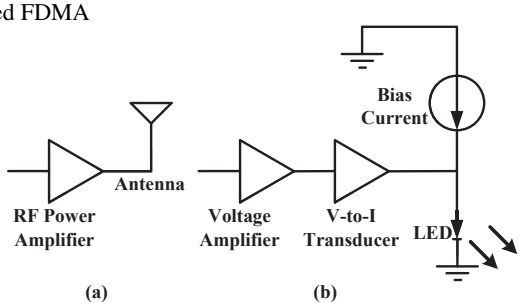

Figure 3 Driving factors: (a) RF communication (b) LED communication

forward current and also to minimize signal clipping and magnitude distortion [8]. The non-linear transfer characteristic also distorts the signals if the biasing point is set on the nonlinear area. Furthermore, the input signals producing forward current larger than the maximum permissible analogue controller forward current are clipped.

3.2. Modified DFT/FFT algorithm and PAPR

The signals d_m after data repacking and received signal x_l are real signals. A widely used FFT algorithm for real sequence can be used in these parts to reduce the complexity of hardware design. Assuming $g(n)$ is a real-valued sequence of $2N$ points. We outline the equations involved in obtaining the $2N$-point DFT (FFT) of $g(n)$ from the computation of one N-point complex-valued DFT. First, we subdivide the $2N$-point real sequence into two N-point sequences as follows:

$$x_1(n) = g(2n), \tag{9}$$

$$x_2(n) = g(2n+1), \tag{10}$$

where $0 \le n \le N-1$. Define the $x(n)$ to be the N-point complex-valued sequence, assuming $1i = \sqrt{-1}$,

$$x(n) = x_1(n) + 1i \cdot x_1(n) \tag{11}$$

The DFT (FFT) of $g(n)$ can be computed using

$$G[k] = X[k]A[k] + X^H[N-k]B[k], \tag{12}$$

where $0 \le k \le N-1$ and $X[N] = X[0]$.

$$A[k] = \frac{1 - 1i \cdot e^{-j2\pi \frac{k}{2N}}}{2}, \tag{13}$$

$$B[k] = \frac{1 + 1i \cdot e^{-j2\pi \frac{k}{2N}}}{2}, \tag{14}$$

This algorithm has been widely used in hardware design of electronic circuit. Utilizing this algorithm can reduce almost half of the complexity of calculation.

In our research, a raised-cosine pulse filter is used for pulse shaping, which is defined as the following in the time domain [7]. In (15), T is the symbol period time and α is the roll-off factor which ranges between 0 and 1.

$$r(t) = \sin\left(\frac{\pi t}{T}\right) = \frac{\cos\frac{\pi\alpha t}{T}}{1 - \frac{4\alpha^2 t^2}{T^2}}. \tag{15}$$

The PAPR of the transmit signal can be expressed as

$$\text{PAPR} = \frac{\max|x(t)|^2}{\frac{1}{NT}\int_0^{NT}|x(t)|^2 dt}. \tag{16}$$

Without pulse shaping, that is, using rectangular pulse shaping, symbol rate sampling will give the same PAPR as the continuous case since the SC-FDMA signal is modulated over a single carrier. Thus, PAPR without pulse shaping with symbol rate sampling can be expresses as follows

$$\text{PAPR} = \frac{\max|x(t)|^2}{E\left[|x(t)|^2\right]}. \tag{17}$$

4. Simulation results and discussions

We have evaluated the detrimental effects of Rayleigh fading channel and AWGN noise over the SC-FDMA system for the QAM modulation schemes (QPSK, 16-QAM). In the simulations, the total number of subcarriers N is set to 256, input data block size M is set to 64, thereby the spreading factor Q is 4. The clipping model is used to model the non-linearity of the emitting diode characteristic. Two situations have been considered: The LED clips the peak power signals on the level of $3dB$ and $12dB$ which means the signals will be clipped when the envelope of the power is greater than the average power $3dB$ and $12dB$, respectively.

The nonlinear effect of the optical wireless channels is modeled using Rapp model [10]. The Rapp's model is a common model for nonlinear transmit amplifiers. This does not model the phase change at all, but defines the amplitude gain as the following

$$g(A) = \frac{A}{(1 + (A)^{2p})^{\frac{1}{2p}}}, \tag{18}$$

where A is input signal amplitude and $g(A)$ is output signal amplitude. p is a nonlinearity parameter, which is set to be 2 in following simulations. The relationship of input and output is illustrated in Figure 4. The effect of the nonlinear amplifier depends on the operating point, which position is defined by its back-off. Input back-off (IBO) and output back-off (OBO) are two common parameters to specify the nonlinear distortion. IBO represents the ratio between the saturated and averaged input power, and

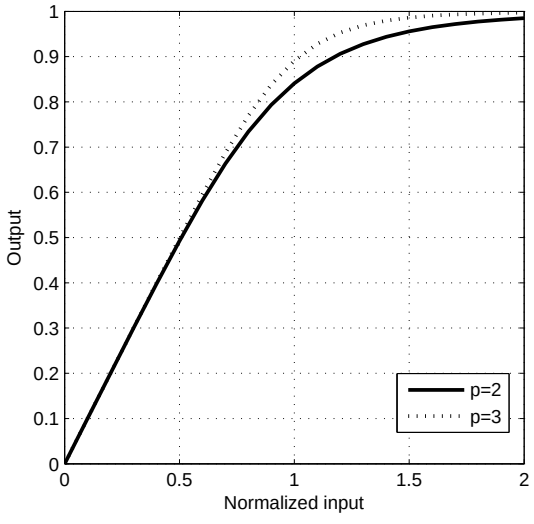

Figure 4 Amplitude input-output transfer curve of the normalized Rapp's model

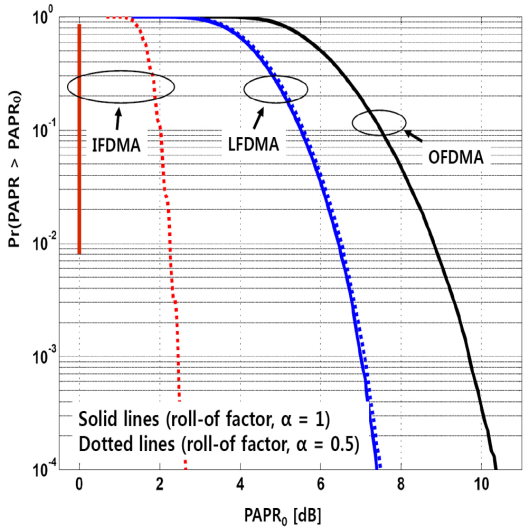

Figure 5 Comparison of CCDF of PAPR for IFDMA, LFDMA, and OFDMA with QPSK

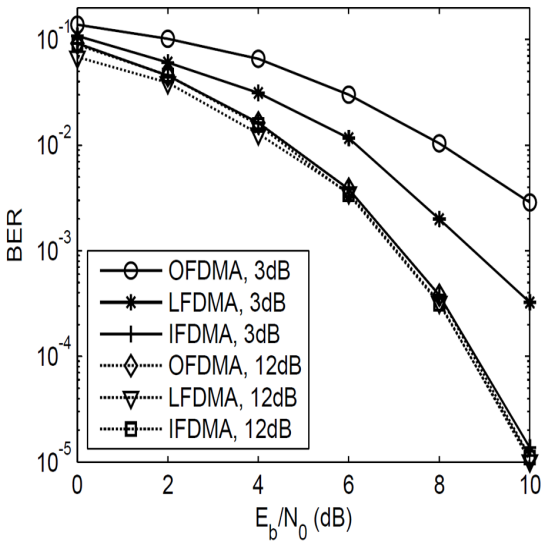

Figure 6 BER performances of WLED systems with various schemes, power clipping at 3dB and 12dB, QPSK

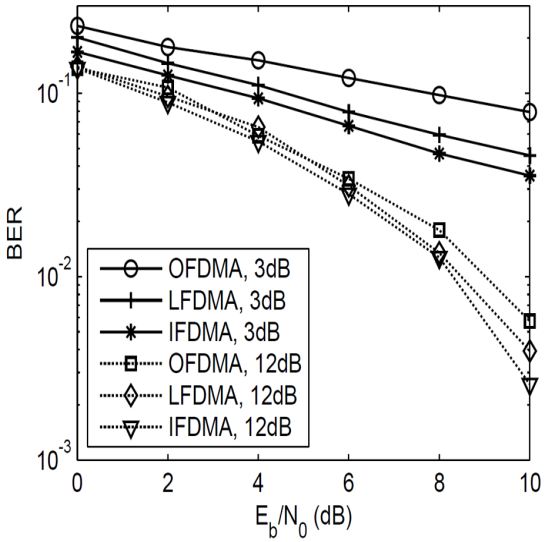

Figure 7 BER performances of WLED systems with various schemes, power clipping at 3dB and 12dB, 16-QAM

that can be expressed as the following

$$\text{IBO} = 10\log_{10}\frac{P_{\max,in}}{\overline{P}_x} \tag{19}$$

and OBO represents the ratio between the saturated and average output power that can be defined as the following

$$\text{OBO} = 10\log_{10}\frac{P_{\max,out}}{\overline{P}_y} \tag{20}$$

Complementary cumulative distribution function (CCDF) of PAPR, which shows the probability that the PAPR is higher than a certain PAPR value PAPR_0, that is Pr[PAPR> PAPR_0], is calculated by Monte Carlo simulation. In the CCDF figures, the lower curves outperform upper curves. The CCDFs of PAPR for IFDMA, LFDMA and in the case of OFDMA was assumed. Raised cosine filter and 8 times oversampling was used when calculating PAPR. Note that no pulse shaping was applied in the case of OFDMA.

When QPSK modulation scheme is adopted, the plots of CCDF of PAPR for IFDMA, LFDMA, and OFDMA are shown in Figure 5. First, in case of no pulse shaping, IFDMA has lower PAPR than the case of OFDMA by almost $9dB$ and LFDMA has lower PAPR than that of OFDMA $2.5dB$ approximately, with the probability of PAPR exceeded the PAPR_0 less than 0.1%. With raised-cosine pulse shaping with roll off factor of 0.5, it can be known from the figure that PAPR increases significantly of IFDMA whereas PAPR of LFDMA hardly increases. Both IFDMA and LFDMA are showing lower PAPR than OFDMA consistently. As aforementioned, the LFDMA has more feasibility than IFDMA in practical system design. For multi-user VLC system, the different user occupies different subcarriers. These subcarriers can be considered as frequency block, and few overhead of pilot symbols or reference signals can obtain the accurate channel state information by utilizing the frequency correlation of the channels. On the other hand, for IFDMA, the user's data is spanned through the all bandwidth and the frequency correlation is useless to estimate the adjacent channel. The overhead of channel estimation and feedback become design problems.

Figure 6 and 7 show the BER performances of proposed schemes and VLC system employing OFDMA technique. We plot the theoretical performance of both IFDMA and LFDMA system. Figure 6 shows the link level performances of WLED communication system with QPSK modulation. The signal is clipped due to WLED device's characteristic. It is observed that when the clipping occurs at $12dB$ level above the normalized power, the performance degrades slightly because the probability of peak power exceeds $12dB$ level is small. However, the performance degrades significantly when clipping occurs at $3dB$ level. Figure 7 shows the similar results while the digital signals are modulated by 16-QAM. The performance degrades slightly when the clipping occurs at $12dB$ level and it degrades significantly when clipping occurs at $3dB$ level. On the other hand, all performances of 16-QAM degrade due to the power per bit degrades comparing to the system which modulated by QPSK. This is because the 16-QAM is not constant modulation, and it introduces some level of PAPR.

In the simulations above, the clippings generates both in-band and out-band frequency components which take effects to the orthogonality between subcarriers, therefore the BER performances degrade a lot. In any situation above, the WLED communication system with SC-FDMA technique outperforms that with OFDMA.

5. Conclusions

A visible light wireless communication prototype has developed. The transmission is based on the assumptions of optical Rayleigh fading channel and AWGN channel, the amplifier at the transmitter is assumed to be nonlinear. We demonstrated that the white LED based visible light data transmission system employing the SC-FDMA multiplexing method, is indeed technically feasible. The low PAPR property of the SC-FDMA technique makes the LED based VLC system to avoid nonlinear distortion which leads better performances than OFDMA-employed system in nonlinear channel, and low peak power driving LED protects human's eye.

Acknowledgement

This research was supported by Basic Research Program through the National Research Foundation of Korea (NRF) funded by the Ministry of Education, Science and Technology (2012R1A1B6002111).
The authors are grateful to the anonymous referee for a careful checking of the details and for helpful comments that improved this paper.

References

[1] T. Komine and M. Nakagawa, IEEE Transactions on Consumer Electronics **50**, 100-107 (2004).
[2] J.H. Kim, C.G. Lee and C.S. Park, Proc. International Society for Optical Engineering **6353**, 635340 (2006).
[3] Y. Tanaka, T. Komine, S. Haruyama, and M. Nakagawa, Proc. 12th IEEE ISPMR 2001 **2**, 81-85 (2001).
[4] M.Z. Afgani, H. Haas, H. Elgala, and D. Knipp, Proc. 2nd TRI-DENTCOM 2006, 129-134 (2006).
[5] H. Elgala, R. Mesleh, H. Haas, and B. Pricope, Proc. 65th IEEE VTC 2007 spring, 2185-2189 (2007).
[6] H.G Myung, J. Lim, and D.J. Goodman, IEEE Vehicular Technology Magazine **1**, 30-38 (2006).
[7] H. Elgala, R. Mesleh, and H. Haas, IEEE WOCN09, 1-5 (2009).
[8] T.S. Rappaport, Wireless Communications: Principles and Practice, Prentice Hall, (2002).
[9] H.G. Myung, J. Lim, and D.J. Goodman, Proc. IEEE PIMRC06, 1-5 (2006).
[10] C. Rapp, Proc. Second European Conference on Satellite Communications, 179-184 (1991).

Young-Ju Kim received the Ph.D degree in Electrical Engineering from Korea Advanced Institute of Science and Technology, Republic of Korea, in 2001. He has been with LG electronics again in UMTS Research Center, Republic of Korea, where he is a senior researcher from 2001 to 2003. Since 2003, he has been with the Department of Information and Communication Engineering at Chungbuk National University, Republic of Korea, where he is now an Associate Professor. His research interests include LTE-Advanced standardization and distributed antenna system design.

Xun Li received the Ph.D degree in Information and Communication Engineering from Chungbuk National University, Cheongju, Republic of Korea, in 2013. Now, he is researcher in Research & Innovation Center, Alcatel-Lucent Shanghai Bell, Shanghai, China. His research interests are in the areas of multiple antennas systems, OFDM, signal processing, etc. He is also interested in next generation communication technique in LTE-Advanced standardization.